Analytical Model for Permanent Magnet Motors With Surface Mounted Magnets

Amuliu Bogdan Proca, *Member, IEEE*, Ali Keyhani, *Fellow, IEEE*, Ahmed EL-Antably, *Member, IEEE*, Wenzhe Lu, *Student Member, IEEE*, and Min Dai, *Student Member, IEEE*

***Abstract*—This paper presents an analytical method of modeling permanent magnet (PM) motors. The model is dependent only on geometrical and materials data which makes it suitable for insertion into design programs, avoiding long finite element analysis (FEA) calculations. The modeling procedure is based on the calculation of the air gap field density waveform at every time instant. The waveform is the solution of the Laplacian/quasi -Poissonian field equations in polar coordinates in the air gap and takes into account slotting. The model allows the rated performance calculation but also such effects as cogging torque, ripple torque, back-emf form prediction, some of which are neglected in commonly used analytical models.**

***Index Terms*—Analytical models, finite element analysis, permanent magnet synchronous motor design.**

I. Introduction

PERMANENT magnet synchronous motors (PMSM) have been around for many years, especially for low power applications, such as servomotors and alternators. Their main advantage, over comparable motors, is the absence of the excitation winding.

The design of permanent magnet motors requires a series of iterative computations based on the selection of different configurations. These include the choice of geometrical dimensions, materials, parameter calculations, etc. The designer needs to assume certain dimensions and materials and then calculate the performance of the designed motor. The performance is then compared with the desired specification. If the specifications are not satisfied, the designer has to modify the design to improve the performance of the motor. Most designers use empirical relations for motor parameters or simplified analytical models in the early stages of the design and then use finite element analysis (FEA) in second stages of the design for better performance evaluation.

The air gap magnetic field density provides valuable information in evaluating motor performance. Knowledge of the field density will not only allow rated performance calculation but also calculation of such effects as cogging torque, ripple torque, back-emf shape, etc. Although the common method of obtaining the air gap field density waveform is FEA, it is time-consuming even on powerful computers and it is difficult to be inserted in an iterative design procedure. It is therefore desirable to use alternative methods to evaluate the air gap field density. Previous efforts were concentrated mainly on evaluating the field density of the permanent magnets. Miller [4] proposes a method of analytically calculating the EMF shape from geometrical data based on BLv formula. The method is based on the single tooth coil rather then a full pitch coil. Sebastian [5] calculates the air gap field density using FEA and assuming a constant airgap (based on the fact that the rotor is skewed) corrected by Carter's coefficient and then finds an empirical formula to describe its shape. Then the flux is calculated by integrating on a surface as a function of the rotor angle. J. de la Ree and Boules [6] assume the flux density in the air gap as known (from FEA) and develop a method of studying the cogging and ripple torque for surface mounted and buried permanent magnet motors. In [7], Boules develops a model for the permanent magnet motor in rectangular coordinates and uses an equivalent pole-arc to correct the variation of the circumferential depth of the magnet with the radius. Other analytical models for the magnetic field density in the air gap were presented in [8]–[13]. Their major drawback is that they do not account for the effect of slotting and they consider the recoil permeability of the permanent magnets to be equal to one. The most recent method was reported by Zhu, Howe [1]–[3] and consisted in solving Laplacian/quasi -Poissonian field equations in polar coordinates on the air gap of the PM machine. The effect of slotting is taken into account using either a 1-d model (the variable being the angular position) or a 2-d model (dependent on both the angular position and the radial position). Their approach is used in the present paper, but, rather then focussing only on the air gap field density, derivations for cogging torque, electromagnetic torque and back-emf shape are also performed.

II. Permanent Magnet Motor Model Using the Air Gap Field Density

Fig. 1 represents the permanent magnet model used in this paper for phase A. Similar models are used for the other two phases. The voltage EA represent the self-inducted voltage of phase A whereas EB and EC represent the voltages mutually generated by phases B and C. EPM represents the voltage generated by the rotating permanent magnets fields on phase A. The

Manuscript received November 22, 2002. This work was supported in part by Delphi Automotive Systems and the National Science Foundation under Grant ECS-9625662.

A. B. Proca is with Solidstate Controls Inc., Columbus, OH 43085 USA (e-mail: bproca@solidstatecontrolsinc.com).

A. Keyhani, W. Lu, and M. Dai are with the Department of Electrical Engineering, The Ohio State University, Columbus, OH 43210 USA (e-mail: keyhani.1@osu.edu; lu.140@osu.edu; dai.21@osu.edu).

A. El-Antably is with Allison Transmission, Indianapolis, IN 46250 USA.

Digital Object Identifier 10.1109/TEC.2003.815829

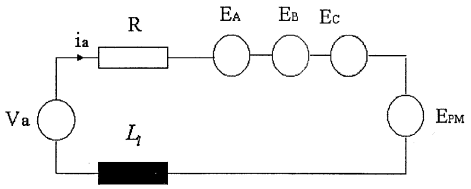

Fig. 1. PM motor model per phase.

above voltages can be expressed as

$$E_A = \sum_{j=1}^{\frac{Ns}{3}} \left(\sum_{i=1}^{N_{coils}} B_{A_{ij}} \cdot L \cdot v \right) \tag{1}$$

$$E_B = \sum_{j=1}^{\frac{Ns}{3}} \left(\sum_{i=1}^{N_{coils}} B_{B_{ij}} \cdot L \cdot v \right) \tag{2}$$

$$E_C = \sum_{j=1}^{\frac{Ns}{3}} \left(\sum_{i=1}^{N_{coils}} B_{C_{ij}} \cdot L \cdot v \right) \tag{3}$$

$$E_{PM} = \sum_{i=1}^{\frac{Ns}{3}} (B_{PM_i} \cdot L \cdot v) \tag{4}$$

where Ns is the total number of slots, N_{coils} is the number of coils per phase, L is the length of the rotor, and v is its speed. It is assumed that the phase resistance R can be easily calculated from the winding data. The leakage inductance (L_l) is approximated as in [14] and is of little interest in this study. In the first equation, B_{Aij} represents the average instantaneous magnetic field density created by coil i of phase A in slot j of phase A. Equations (2) and (3) are represented in a similar fashion. In the fourth equation, B_{PMi} represents the average field density created by the permanent magnets on slot i of phase A.

The advantages of using such a model over other existing models is that it can predict parasitic effects in the permanent magnet machine, such as cogging torque, ripple torque, and nonsinusoidal back-emf. To be able to use the above model, knowledge of both the permanent magnet field (B_{PM}) and the armature field (B_A, B_B, B_C) variation as a function of angular position is needed.

III. Assumptions

Certain assumptions have to be taken into account for this model. The magnets are surface mounted and are magnetized radially. The stator slots are either rectangular or trapezoidal as shown in Fig. 2. Also, the following material assumptions were used.

- The ferromagnetic material of the core has a linear B-H curve.
- Saturation is neglected.
- The spacer between the magnets has the same permeability as the magnets.

IV. Permanent Magnet Field

The permanent magnet field density of the motor is affected by slotting. Slotting is dependent on the rotor position and the wave shape of the magnetic field density referred to the rotor also changes with position. In order to obtain a position independent mapping, an approach similar to the one in [3] was used. The authors mapped the air gap field density to the dimensions of the motor assuming a slotless stator. The field density function was then multiplied with the relative air gap permeance function, as described in [3] for a 1-D model. Fig. 2 shows a motor section and the stator and rotor references used throughout this paper.

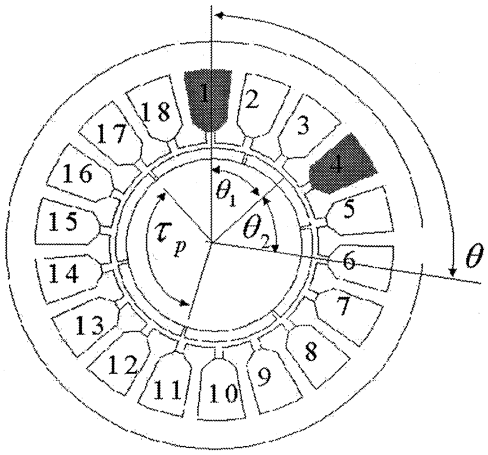

Fig. 2. Cross-section of the motor.

Using the same variables as in the picture, the instantaneous value of the permanent magnet field density in the air gap is

$$\begin{aligned} B_{PM}(\theta) &= B_{PMsless}(\theta_2) \cdot \lambda_{rel}(\theta) \\ &= B_{PMsless}(\theta - \theta_1) \cdot \lambda_{rel}(\theta) \end{aligned} \tag{5}$$

where $B_{PM-sless}(\theta_2)$ is the field density function for a slotless stator, θ is the angular position on the rotor surface, θ_1 is the rotor displacement, and θ_2 is the position referenced to the rotor. λ_{rel} is the relative air gap permeance function that accounts for slotting and is based on the assumption that the magnetic flux lines have semicircular paths in the slots with radii equal to the shortest distance to the tooth edges as shown in Fig. 3.

The relative permeance function can be derived as

$$\lambda_{rel} = \frac{g + \frac{l_m}{\mu_r}}{g + \frac{\pi}{2} w_1 + \frac{l_m}{\mu_r}} \text{at the slots} \tag{6}$$

and $\lambda_{rel} = 1$ outside the slots, where w_1 is the distance between point where the field is evaluated and the closest tooth edge, g is the air gap length, and l_m is the magnet depth. The instantaneous field density distribution of one magnetic pole $B_{PMsless}$ assuming a slotless stator, is calculated as in [1]. The permanent magnet magnetization, shown in Fig. 4 for a pair of poles, is decomposed in a Fourier series of odd terms as follows:

$$M(\theta_2) = \sum_{n=1,3,5...}^{\infty} 2 \cdot \frac{B_r}{\mu_0} \cdot \alpha_p \cdot \frac{\sin\left(\frac{n \cdot \pi \cdot \alpha_p}{2}\right)}{\frac{n \cdot \pi \cdot \alpha_p}{2}} \cdot \cos(n \cdot p \cdot \theta_2) \tag{7}$$

where B_r is the magnetic remanence of the permanent magnet material, $\alpha_p = (\tau_m / \tau_p)$ is the magnet pitch/pole pitch ratio, and p is the number of pair of poles.

By solving the magnetic potential distribution equations in the air gap in polar coordinates [1], an expression for the permanent

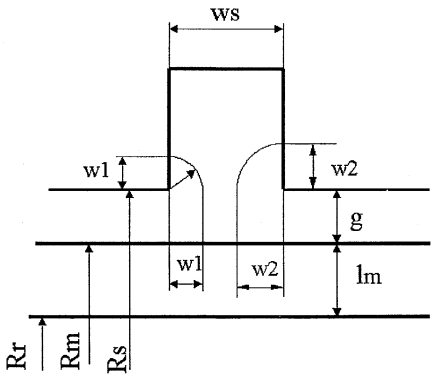

Fig. 3. Approximation of the flux line paths in a slot.

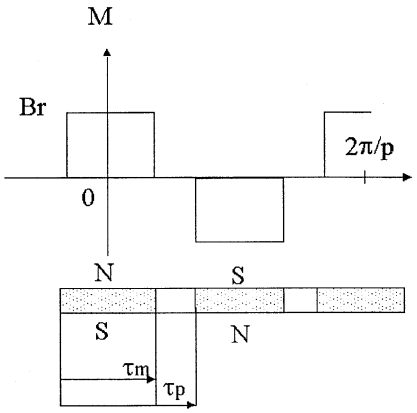

Fig. 4. Magnetization of permanent magnets.

magnet field distribution at the stator surface results: (See equation at the bottom of the page) where R_s is the radius at the stator surface, R_m is the radius at the magnet surface, and R_r is the radius at the rotor core surface and $r = ((R_s + R_m)/2)$. For the case in which the product $np = 1$ (fundamental of the field density of a twp-pole motor), (8) cannot be used. The solution of the magnetic potential distribution equations in the air gap yields

$$B_{PM1}(\theta_2) = \frac{2B_r}{\mu_r} \cdot \frac{\sin\left(\frac{\pi \cdot \alpha_p}{2}\right)}{n\pi} \cdot \left[\frac{\left(\frac{R_m}{R_s}\right)^2 - \left(\frac{R_r}{R_s}\right)^2 + \left(\frac{R_r}{R_s}\right)^2 \cdot \ln\left(\frac{R_m}{R_r}\right)^2}{\frac{\mu_r+1}{\mu_r}\left[1 - \left(\frac{R_r}{R_s}\right)^2\right] - \frac{\mu_r-1}{\mu_r}\left[\left(\frac{R_m}{R_s}\right)^2 - \left(\frac{R_r}{R_m}\right)^2\right]} \right] \cdot \left[1 + \left(\frac{R_s}{r}\right)^2\right] \cos(\theta_2). \quad (9)$$

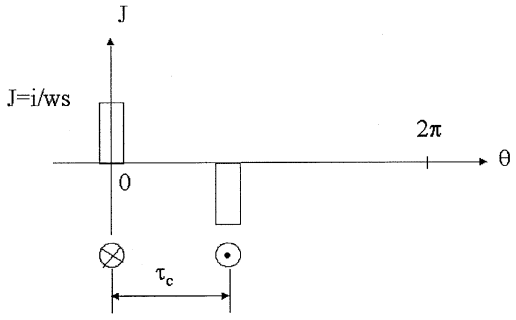

Fig. 5. Current sheet distribution for a coil.

V. Armature Field

The armature field density of one phase can be modeled as a summation of the field densities created by each coil of that phase. For example, the armature field of a phase of a three-phase, six-pole, and 18-slot motor (as shown in Fig. 2) can be derived as

$$B_A(\theta) = B_{1-4}(\theta) + B_{7-10}(\theta) + B_{13-16}(\theta) \quad (10)$$

where the three coils sitting in slots 1 and 4, 7 and 10, and 13 and 16 all contribute to phase A flux density.

To calculate the armature reaction field density of a single coil, the stator is first assumed slotless, and the armature field is calculated. Then the relative permeance function is estimated as in the permanent magnet field section. The product between the slotless stator field and the relative permeance function will provide the expression of the armature reaction field for one coil. For the slotless stator armature field calculation, it is assumed that the current density sheet is uniform along the slot opening, as shown in Fig. 5.

Using the coordinate system of Fig. 2, the Fourier series expansion of the current density sheet results in

$$J(\theta) = \frac{4i}{\pi \cdot w_s} \cdot \sum_{n=1}^{\infty} \frac{1}{n} \sin\left(n \frac{w_s}{2 \cdot R_s}\right) \cos\left(n \cdot \left(\theta - \frac{\tau_c}{2}\right)\right) \quad (11)$$

where I is the instantaneous value of the current, w_s is the slot opening, and τ_c is the coil opening angle. By solving the magnetic potential distribution equations in the air gap in polar coordinates [2], an expression for the armature field density of a

$$B_{PMsless}(\theta_2) = \sum_{n=1,3,5\ldots}^{\infty} \frac{4B_r}{\mu_r} \cdot \frac{\sin\left(\frac{n \cdot \pi \cdot \alpha_p}{2}\right)}{\pi} \cdot \frac{p}{(np)^2 - 1} \cdot \left\{ \frac{(n \cdot p - 1) + 2 \cdot \left(\frac{R_r}{R_m}\right)^{n \cdot p+1} - (n \cdot p + 1) \cdot \left(\frac{R_r}{R_m}\right)^{2n \cdot p}}{\frac{\mu_r+1}{\mu_r}\left(1 - \left(\frac{R_r}{R_s}\right)^{2n \cdot p}\right) - \frac{\mu_r-1}{\mu_r}\left(\left(\frac{R_m}{R_s}\right)^{2n \cdot p} - \left(\frac{R_r}{R_m}\right)^{2n \cdot p}\right)} \right\} \cdot \left[\left(\frac{r}{R_s}\right)^{np-1} \left(\frac{R_m}{R_s}\right)^{np+1} + \left(\frac{R_m}{r}\right)^{np+1}\right] \cdot \cos(np\theta_2) \quad (8)$$

coil (distributed in slots k and l) is obtained

$$B_{kl-sless}(\theta) = \frac{2\mu_0 i}{\pi}\sum_{n=1}^{\infty}\frac{1}{r}\cdot\frac{\sin\left(n\frac{w_s}{2R_s}\right)}{n\frac{w_s}{2R_s}} \cdot\sin\left(\frac{n\tau_c}{2}\right)\cdot\left(\frac{r}{R_s}\right)^n\cdot\frac{1+\left(\frac{R_r}{r}\right)^{2n}}{1-\left(\frac{R_r}{R_s}\right)^{2n}} \cdot\cos\left(n\cdot\left(\theta-\frac{\tau_c}{2}\right)\right) \quad (12)$$

and when slotting is considered

$$B_{kl}(\theta) = B_{kl-sless}(\theta)\cdot\lambda_{rel}(\theta). \quad (13)$$

VI. Torque Calculation

The instantaneous torque can be expressed as the derivative of the co-energy in respect to the rotor-stator position in the air gap

$$T_{el} = \frac{\partial W'}{\partial\theta}. \quad (14)$$

The co-energy can be expressed as

$$W' = W'_{PM} + W'_{pm-el} + W'_{el} \quad (15)$$

where W'_{PM} is the component due only to the PM field (cogging torque), W'_{PM-el} is the component due to the interaction between the armature field and the permanent magnet field (electromagnetic torque) and W'_{el} is the component due to the armature field only (reluctance torque). Assuming that the rotor has no saliency (the filler has the same permeability as the magnets), the third term in the equation is zero. The electromagnetic torque can be calculated as the summation of the torques produced by the current-field interaction at each slot

$$T_{el}(\theta_1) = r\cdot L\sum_{j=1}^{N_s}\int_0^{ws} B_{PM}(w1)\cdot J(w1)dw1. \quad (16)$$

Numerically, the equation becomes

$$T_{el}(\theta_1) = \frac{2\pi r^2 L}{N}\cdot\sum_{m=1}^{N} B_{PM}\left(\frac{2\pi}{N}m+\theta_1\right)\cdot J\left(\frac{2\pi}{N}m+\theta_1\right) \quad (17)$$

where N is the number of samples in which the evaluation is performed

$$J\left(\frac{2\pi}{N}m+\theta_1\right) = \frac{i_a}{ws} \text{ if } \frac{2\pi}{N}m+\theta_1 \text{ is in a phase A slot and the current has positive direction}$$

- $J[(2\pi/N)m+\theta_1] = -(i_a)/(ws)$ if $(2\pi/N)m+\theta_1$ is in a phase A slot and the current has negative direction;
- J is similar for phases B and C;
- $J[(2\pi/N)m+\theta_1] = 0$ if $(2\pi/N)m+\theta_1$ is outside the slot opening.

The ripple in the electromagnetic torque has three main causes. The first is the nonsinusoidal shape of the currents in most brushless dc motors. The second cause is the mismatch in shape between the back-emf shape and the current shape. The third is given by the presence of the stator slots. Equation (17) is able to predict all three causes. However, in our simulations, the currents were presumed sinusoidal, and consequently, the first component will not appear.

The cogging torque is the torque that results from the nonconstant airgap reluctance due to slotting (i.e. due to the tendency of the rotor to align with the low reluctance paths). The torque is produced by the fluxes that enter the teeth walls, as shown in Fig. 3. Using the notations of Fig. 3, the cogging torque expression results into

$$T_{cog}(\theta_1) = \frac{L}{2\cdot\mu_0}\cdot\sum_{m=1}^{N_s}\left[\int_0^{\frac{ws}{2}} B_{PM}^2(w1)\cdot(R_s+w1)dw1 - \int_{\frac{ws}{2}}^{ws} B_{PM}^2(w2)\cdot(R_s+w2)dw2\right]. \quad (18)$$

Numerically, the equation becomes

$$T_{cog}(\theta_1) = \frac{\pi\cdot L\cdot R_s}{2\cdot\mu_0\cdot N}\sum_{m=1}^{N}\left[B_{PM}^2\left(\frac{2\pi}{N}m+\theta_1\right)\cdot(R_M+g_\alpha)\cdot ssg\right] \quad (19)$$

where

$g_\alpha = 0$ and $ssg = 0$	outside the slot opening;
$g_\alpha = w1+g$ and $ssg = 1$	on the left side of the slot opening;
$g_\alpha = w2+g$ and $ssg = -1$	on the right side of the slot opening.

VII. Back-EMF Calculation

The back-emf is the voltage induced in the stator windings by the variable magnetic field in the airgap. There are two common definitions of the back emf in literature. One definition regards the back emf as only the effect of the rotor magnetic field, where as the other one also includes the mutually and self-induced voltage between windings as part of the back emf. In this study, the second definition will be used.

The back emf of one phase can be calculated as the summation of the voltages induced in each coil side of that phase

$$E_A(t) = -\sum_{j=1}^{N_s}\frac{d\phi_j}{dt} = -\sum_{j=1}^{N_s}\frac{d\int_0^{ws} L\cdot B_j(t)dw1}{dt} \quad (20)$$

where ϕ_j is the magnetic flux in slot j. The numerical expression

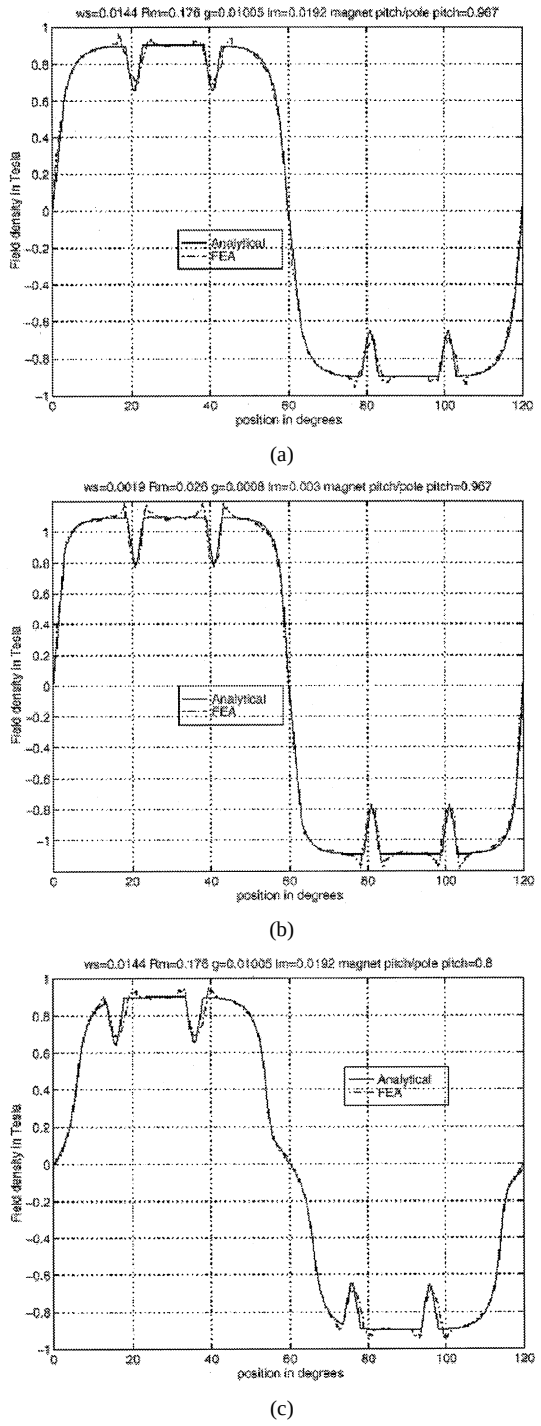

Fig. 6. Comparison with FEA for PM field density.

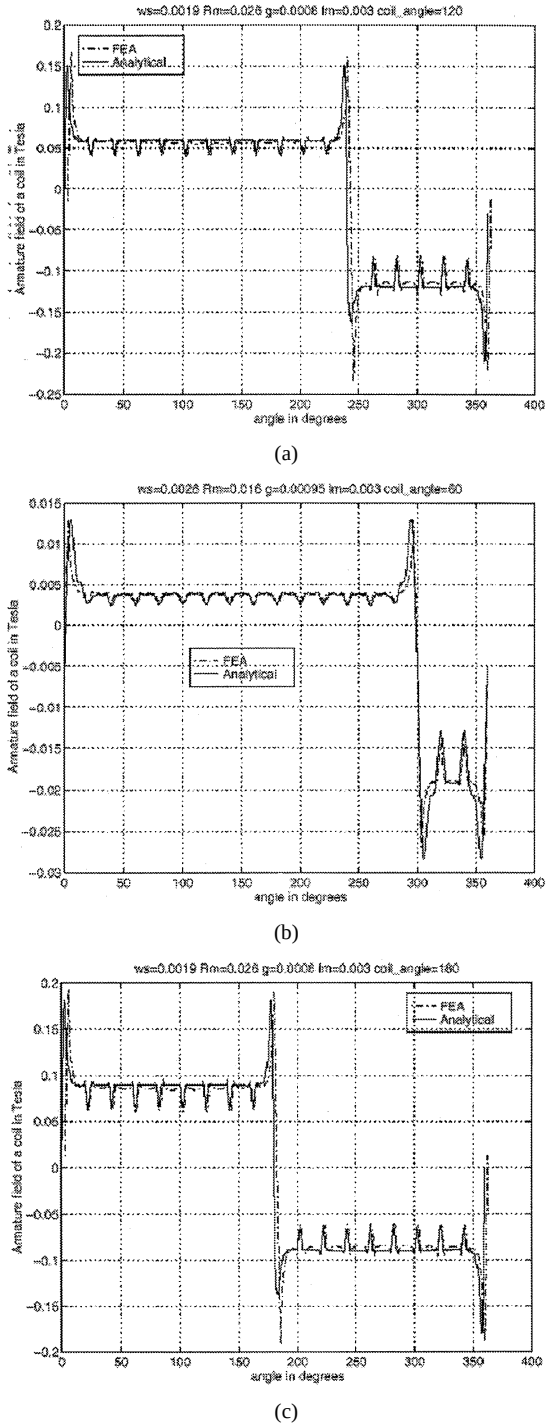

Fig. 7. Comparison with FEA for armature field density.

of the above equation becomes

$$E_A(t) = \frac{L \cdot R_s \cdot \omega \cdot}{N} \sum_{m=1}^{N} \times \left[B_{PM}\left(\frac{2\pi}{N}m + \omega \cdot t\right) + B_A\left(\frac{2\pi}{N}m\right) + B_B\left(\frac{2\pi}{N}m\right) + B_C\left(\frac{2\pi}{N}m\right)\right] \times ssa\left(\frac{2\pi}{N}m\right) \quad (21)$$

where $ssa(\theta) = 1$ if θ is a phase A slot and the direction of the conductor is positive; $ssa(\theta) = -1$ if θ is a phase A slot and the direction of the conductor is negative; $ssa(\theta) = 0$ otherwise.

VIII. Comparison With Finite Element Results

The analytical model developed in this paper was compared with a FEA model. As a test case, a motor with three phases, six poles, and 18 slots was chosen. Fig. 6 shows a comparison between the PM field density in the air gap for various dimensions of the motor.

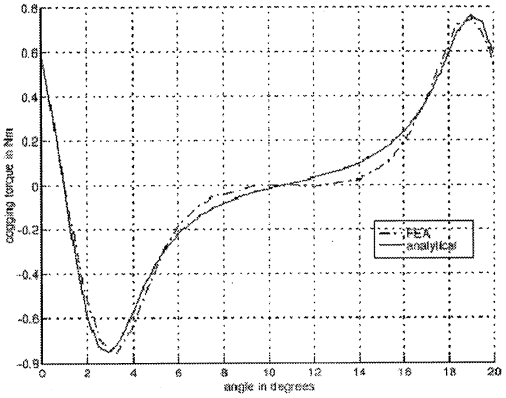

Fig. 8. Comparison with FEA for cogging torque.

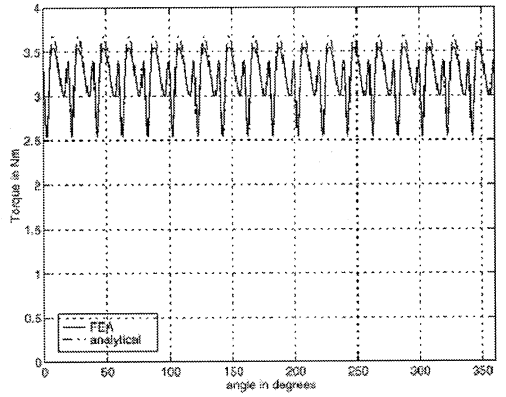

Fig. 9. Comparison with FEA for total torque.

Fig. 7 shows a comparison between the armature reaction field density for various coil angles. Fig. 8 shows a comparison between the cogging torque obtained using FEA and the analytical model for the test case for one slot pitch. Fig. 9 shows a comparison between the total torque (comprising of both electromagnetic and cogging) using FEA and the analytical model. Sinusoidal currents were used in the simulation. A torque angle of 30° was used to emphasize the ripple in the torque function.

IX. Conclusions

A method for modeling permanent magnet motors has been developed in this paper. The model is based on the magnetic field density in the machine air-gap. The model allows the calculation of such effects as cogging torque, ripple torque, back-emf form prediction, and effects usually neglected in commonly used analytical models. The model can be used in an iterative design program and reduces the use of FEA.

References

[1] Z. Q. Zhu, D. Howe, B. Ekkehard, and B. Ackermann, "Instantaneous magnetic field distribution in brushless permanent magnet motors, part I: open-circuit field," *IEEE Trans. Magn.*, vol. 29, pp. 124–134, Jan. 1993.

[2] Z. Q. Zhu and D. Howe, "Instantaneous magnetic field distribution in brushless permanent magnet motors, part II: armature reaction field," *IEEE Trans. Magn.*, vol. 29, pp. 136–142, Jan. 1993.

[3] ——, "Instantaneous magnetic field distribution in brushless permanent magnet motors, part III: effect of stator slotting," *IEEE Trans. Magn.*, vol. 29, pp. 143–151, Jan. 1993.

[4] T. J. E. Miller and R. Rabinovici, "Back-EMF waveforms and core losses in brushless DC motors," in *Proc. Inst. Elect. Eng. Elect. Power Applicat.*, vol. 141, May 1994, pp. 144–154.

[5] T. Sebastian and V. Gangla, "Analysis of induced EMF waveforms and torque ripple in a brushless permanent magnet machine," *IEEE Trans. Ind. Applicat.*, vol. 32, pp. 195–200, Jan./Feb. 1996.

[6] J. de la Ree and N. Boules, "Torque production in permanent-magnet synchronous motors," *IEEE Trans. Ind. Applicat.*, vol. 25, pp. 107–112, Jan./Feb. 1989.

[7] N. Boules, "Two dimensional field analysis of cylindrical machines with permanent magnet excitation," *IEEE Trans. Ind. Applicat.*, vol. IA-20, pp. 1267–1277, Mar. 1984.

[8] G. R. Slemon, "On the design of high-performance surface-mounted PM motors," *IEEE Trans. Ind. Applicat.*, vol. 30, pp. 134–140, Jan./Feb. 1994.

[9] Q. Gu and H. Gao, "Airgap field for PM electrical machines," *Electrical Machines and Power Systems*, vol. 10, pp. 459–470, 1985.

[10] T. Sebastian and M. A. Rahman, "Modeling of permanent magnet synchronous motors," *IEEE Trans. Magn.*, vol. MAG-22, pp. 1069–1071, Sept. 1986.

[11] J. Y. Hung and Z. Ding, "Design of currents to reduce torque ripple in brushless permanent magnet motors," in *Proc. Inst. Elect. Eng.–Elect. Power Applicat.*, vol. 140, July 1993, pp. 260–266.

[12] M. A. Alhamadi and N. A. Demerdash, "The dimensional magnetic field computation by a coupled vector-scalar potential method in brushless DC motors with skewed permanent magnet mounts—the no-load and load results," *IEEE Trans. Energy Conversion*, vol. 9, pp. 15–22, Mar. 1994.

[13] H. R. Bolton, Y. D. Liu, and N. M. Mallinson, "Investigation into a class of brushless DC motor with quasisquare voltages and currents," in *Proc. Inst. Elect. Eng.–Elect. Power Applicat.*, vol. 133, Mar. 1986, pp. 103–111.

[14] D. C. Hanselman, *Brushless Permanent-Magnet Motor Design*. New York: McGraw-Hill, 1994.

Amuliu Bogdan Proca (S'96–M'01) received the M.S.E.E. and Ph.D. degrees in electrical engineering from The Ohio State University, Columbus, in 1997 and 2001, respectively.

Currently, he is with Solidstate Controls, Inc., Columbus. His research interests include electric machines control, modeling, parameter estimation, and design.

Ali Keyhani (S'72–M'76–SM'89–F'98) received the Ph.D. degree from Purdue University, West Lafayette, IN, in 1975.

Currently, he is a Professor of Electrical Engineering at The Ohio State University, Columbus. From 1967 to 1969, he was with Hewlett-Packard Co., Palo Alto, CA, involved in the computer-aided design of electronic transformers. From 1970 to 1973, he was with Columbus and Southern Ohio Electric Co. in computer applications for power system engineering problems. In 1974, he joined TRW Controls and worked on the development of computer programs for energy control centers. From 1976 to 1980, he was a Professor of Electrical Engineering at Tehran Polytechnic, Tehran, Iran. His research interests include control and modeling, parameter estimation, failure detection of electric machines, transformers, and drive systems.

Ahmed EL-Antably (M'02) received the M.S. degree in control engineering and the Ph.D. degree in electrical engineering from the University of Sussex, U.K., in 1975 and 1980, respectively.

Currently, he is with Allison Transmission, Indianapolis, IN. He worked in various oil fields pumping stations from 1968 to 1973. He was also with Westinghouse Electric Corporation from 1980 to 1989, involved in the design, analysis, manufacturing, testing, and service of electric drive motor systems. He is the author of 15 publications and the holder of four patents.

Wenzhe Lu (S'00) received the B.S. degree from Xi'an Jiaotong University, Xi'an, China, in 1993, and the M.S. degree from Tsinghua University, Beijing, China, in 1996. He is currently pursuing the Ph.D. degree in electrical engineering at The Ohio State University, Columbus.

His research interests include modeling and control of switched reluctance motors for electric vehicle applications.

Min Dai (S'99) received the B.S. and M.S. degrees in electrical engineering from Tsinghua University, Beijing, China, in 1994 and 1997, respectively, and the M.S. degree in computer science from the University of Alabama, Huntsville, in 1999.

He joined the Department of Electrical Engineering at The Ohio State University, Columbus, in 1999. His current research interests include electrical machines and variable speed drives, power electronics, and distributed power system control.